Supporting Information

Multi-responsive, Bidirectional and Large Deformation Bending Actuators Based on Borax Crosslinked Polyvinyl Alcohol Derivative Hydrogel

Liang Gao,[*] Guoqiang Guo, Mengjuan Liu, Zeguo Tang, Liangxu Xie[†]*, Yanping Huo[*]

School of Chemical Engineering and Light Industry, Guangdong University of Technology, Guangzhou, China

[*]*Corresponding to Dr. Liang Gao (gaoliang@gdut.edu.cn) or Dr. Liangxu Xie (xlxhku@gmail.com) or* Yanping Huo *(yphuo@gdut.edu.cn)*

Supporting Note I: Actuator modeling

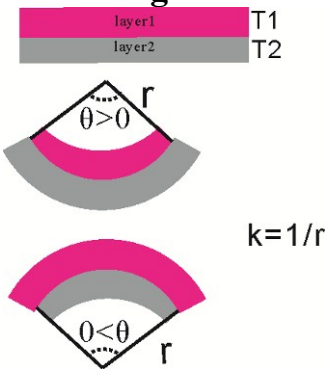

Figure. S1. Schematic illustration of bilayer PVA-DEEDA-Borax hydrogel actuator. Pink layer stands for PVA-DEEDA-Borax, while gray layer stands for BOPP substrate.

The bilayers of our HA are PVA-DEEDA-Borax and BOPP (**Figure S1**). According to the literatures[1], the curvature of the actuator can be calculated from **Eq. S1** as follows:

$$\mathrm{k}=\frac{1}{r}=\frac{6E_1E_2t_1t_2(t_1+t_2)((\alpha_2-\alpha_1)\Delta T-\beta\Delta C)}{(E_1t_1^{\,2})^2+(E_2t_2^{\,2})^2+2E_1E_2t_1t_2(2t_1^{\,2}+3t_1t_2+2t_2^{\,2})} \quad \textbf{(Eq. S1)}$$

Where t_1 and t_2 are respective thickness, modules of PVA-DEEDA-Borax and BOPP, respectively; β is the coefficient of hygroscopic expansion of PVA-DEEDA-Borax; ΔC is the change of moisture concentration in PVA-DEEDA-Borax (Here, the hygroscopicity of BOPP is negligible); ΔT is the temperature change; α_1 and α_2 are the respective coefficient of

thermal expansion for the PVA-DEEDA-Borax and BOPP film; Clearly, α_1 should be negative; therefore, the shrinkage of PVA-DEEDA-Borax upon heating indeed contributes to the performance of bending.

Supporting Note II Optimization of the PVA-DEEDA-Borax/BOPP bilayer actuator.

We noted that two key factors play critical role in affecting the bending of our HA device, including (1) thickness of active layer and (2) the addition amount of borax in the PVA-DEEDA. To optimize the actuation, we mainly concern the bending towards BOPP side (angle <0, see **Figure 1b** in main text). Since mechanical strength of hydrogel generally decreases along with the increase on water content, it can be expected that the bending of PVA-DEEDA-Borax-based actuator toward BOPP layer is more challenging than that at lower humidity. We therefore mainly optimize the actuator under high humidity (82.1%) and low temperature (10 ^{o}C).

(1)*Thickness Effects of PVA-DEEDA-Borax layer*

As it has been known, the thickness ratio between substrate and active layer significantly influence the bending of bilayer actuator.[2] Indeed, as indicated in **Figure S4-S5**, when the thickness ratio of PVA-DEEDA-Borax layer to BOPP substrate is smaller than 1.82, the actuation cannot maintain its negative bending angle towards BOPP side. Thus, sufficient thickness of PVA-DEEDA-Borax layer is necessary. When the thickness increase to 1.82, the bending angle reaches -360^{o} and remains shape for at least 2 h (**Figure S5**). Further increasing the thickness of active layer cannot result in significant improvement on the bending degree, but slightly enhanced kinetics is observed. Considering lighter actuator is more efficient and

energetic to do work, we therefore choice the actuator with thickness ratio of 1.82 for further performance study.

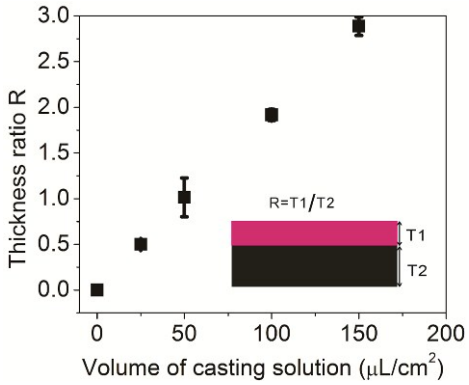

Figure S2. The thickness of ratio of PVA-DEEDA-Borax active layer to substrate as a function of volume of casting solution.

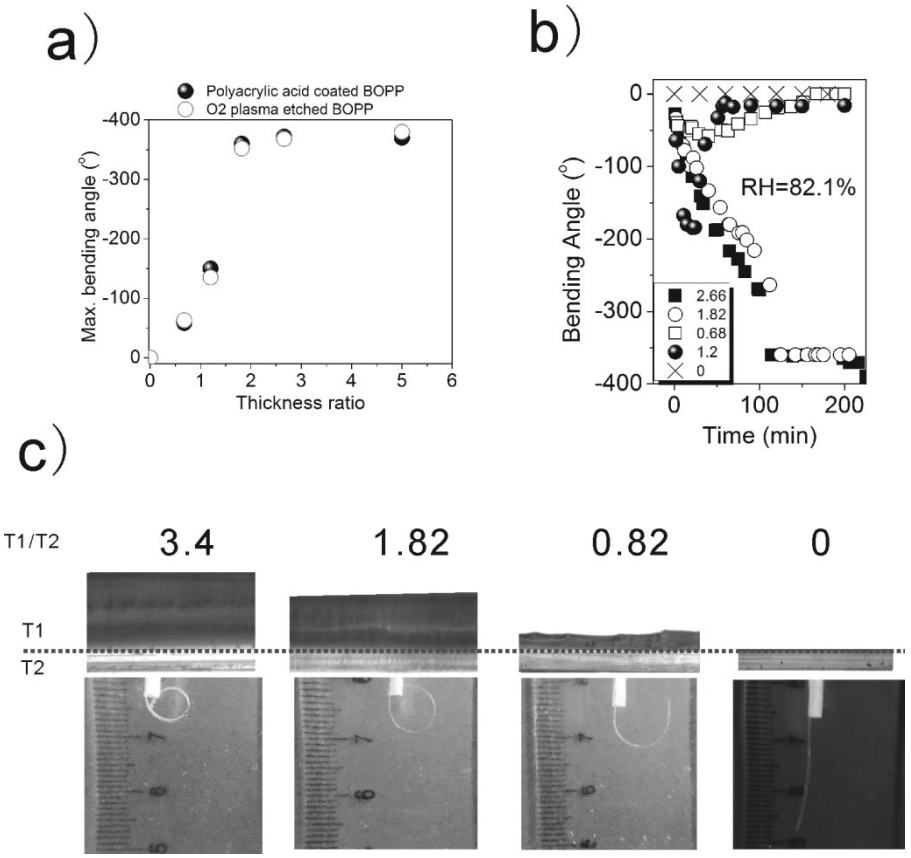

Figure S3. (a) The bending angle of PVA-DEEDA-Borax actuator at RH=82.1% as a function of thickness ratio of PVA-DEEDA-Borax layer to polyacrylic acid coated and O2

plasma etched BOPP layer; (b) the bending kinetics of PVA-DEEDA-Borax/polyacylic acid coated BOPP; (c) Image of thickness (optical microscopy) and max. bending angle (digital camera).

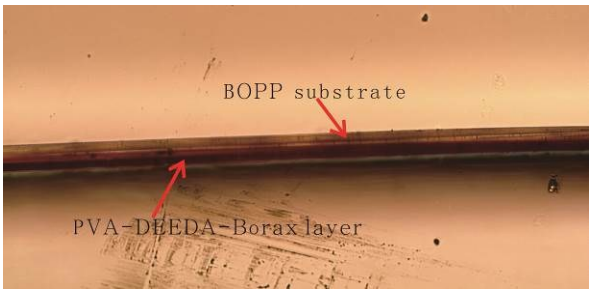

Figure S4. The photo microscopic image of cross section of PVA-DEEDA-Borax-based actuator.

(2) *Amount effects of borax*

We also note that the addition amount of borax also plays very key effect on the bending of our HA. As shown in **Figure S4** as below, PVA-DEEDA without addition of borax barely shows bending at 10 ^{o}C and 82% RH. As the addition amount of borax increases to 10 wt.%, the actuator bends to the opposite direction of BOPP due to the expansion of PVA-DEEDA-1Borax layer. Interestingly, further increasing the dose of borax somehow causes the deterioration of performance as indicated by the less bending behavior (**Figure S4c**).

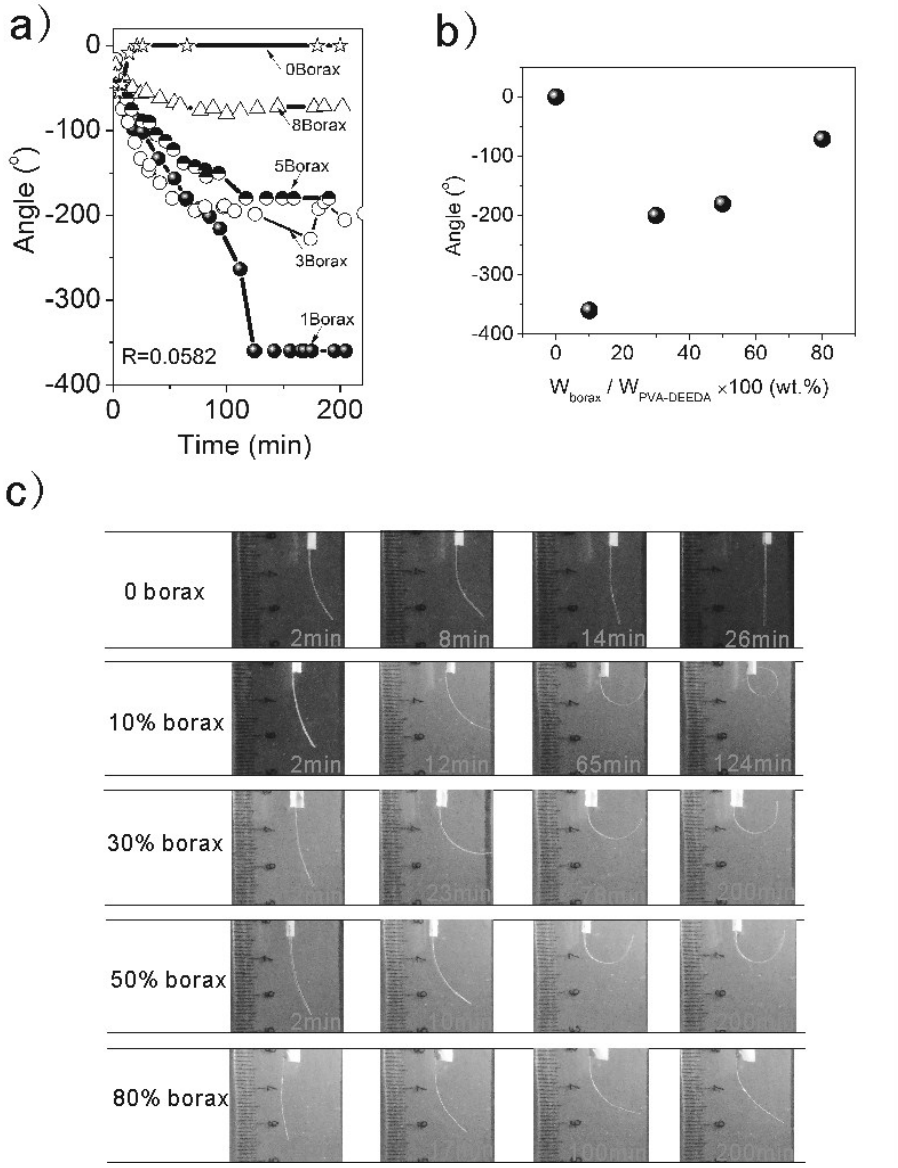

Figure S5. Borax amount effect on the (a) Bending kinetics, (b) max bending angle and (c) physical observation of the actuation of HA constructed by PVA-DEEDA crosslinked by various amount of borax.

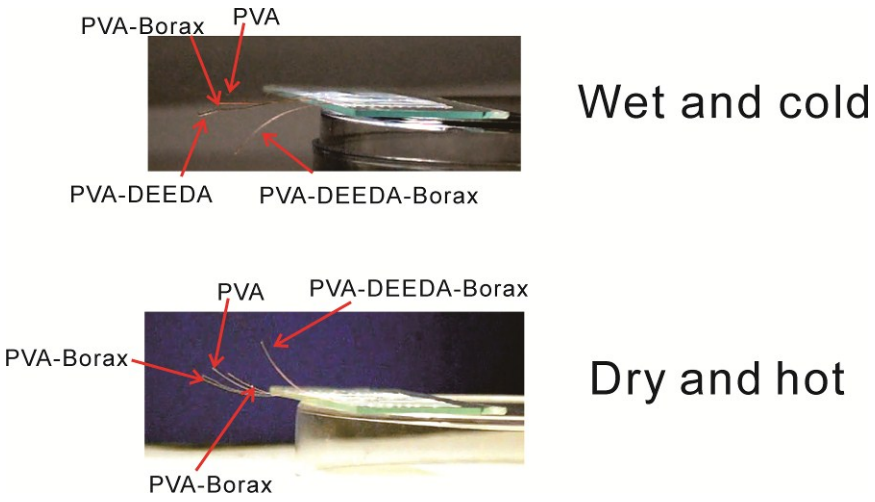

Figure S6. The bending angle of HAs constructed by using PVA, PVA-Borax, PVA-DEEDA, PVA-DEEDA-Borax. The "wet and cold" refers to an environment inside a refrigerator; while the "dry and hot" refers to an environment inside an hot oven.

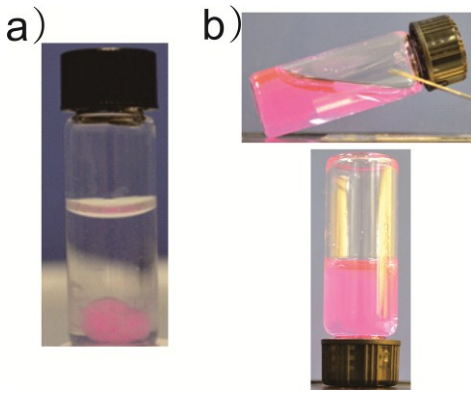

Figure S7. The images of adding borax to (a) 2.5 wt.% PVA-DEEDA solution; (b) 1 wt.% PVA-DEEDA solution at 20 ^{o}C. A drop RhB solution was added to increase the observability. The obtained PVA-DEEDA-Borax solution shows thermally responsive gelation behavior (**Figure S2**).

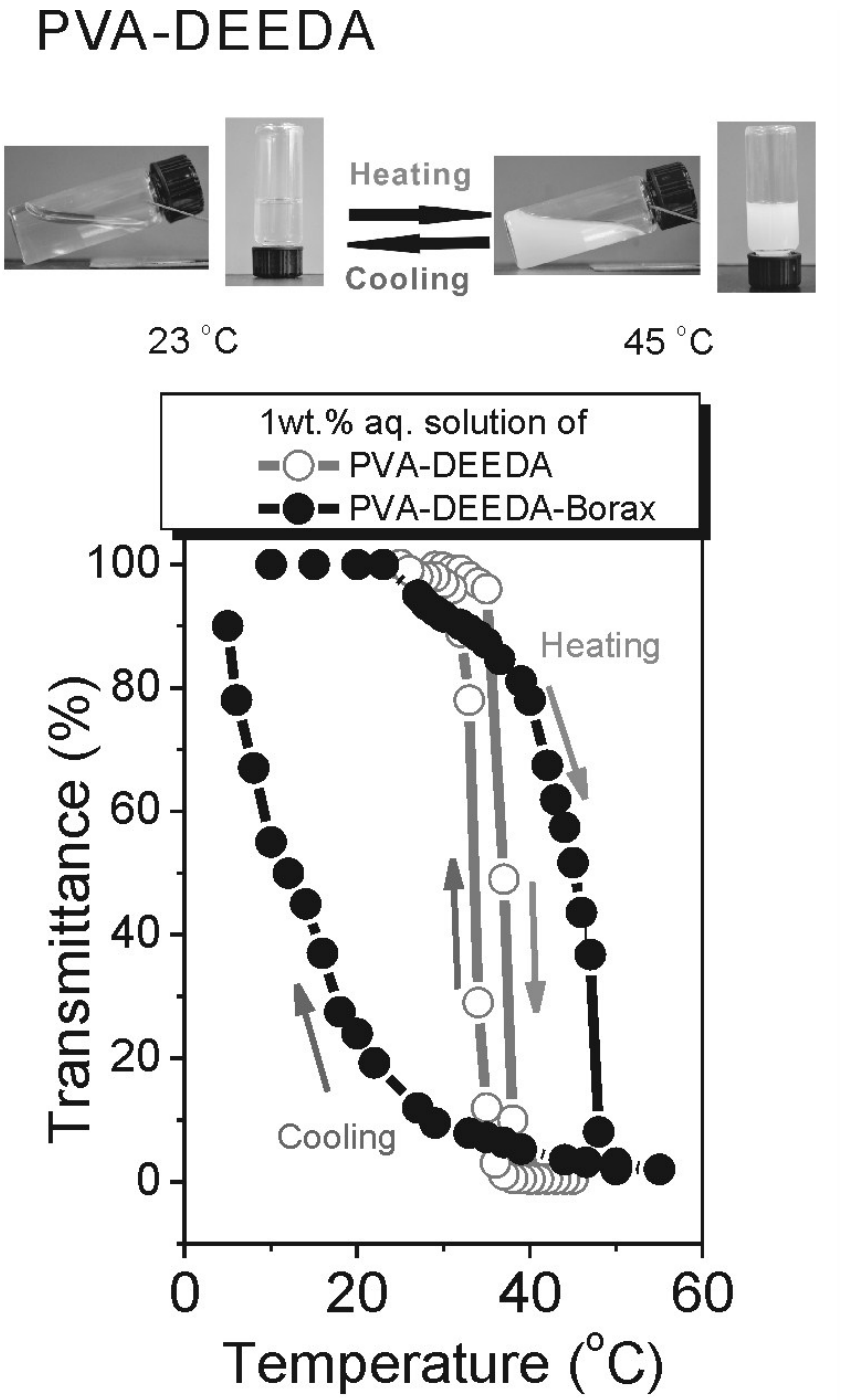

Figure S8. (a) The gelation process of PVA-DEEDA-borax; (b)Uv-vis of PVA-DEEDA+Borax and PVA-DEEDA.

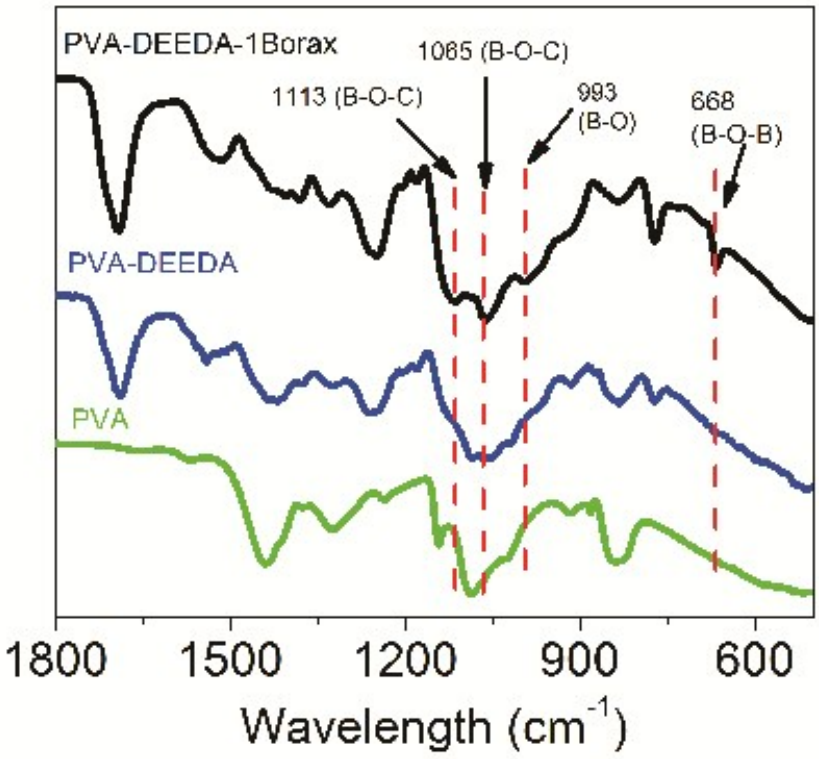

Figure S9. ATR-FTIR of PVA, PVA-DEEDA and PVA-DEEDA-Borax.

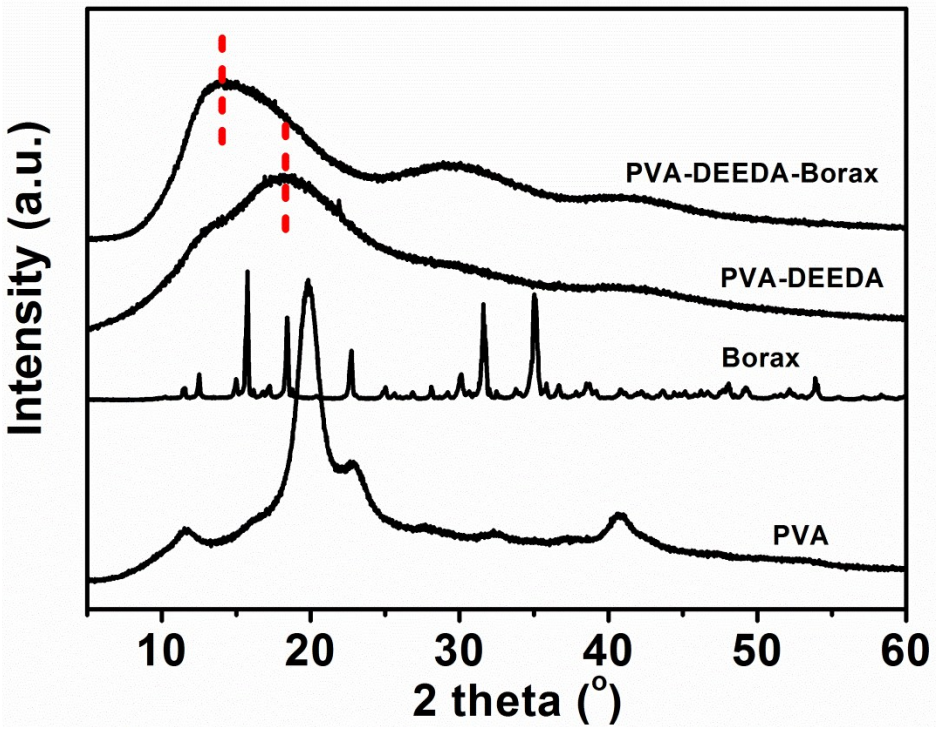

Figure S10. XRD of PVA, borax, PVA-DEEDA and PVA-DEEDA-Borax. Interestingly, with comparison to the pristine PVA-DEEDA, crosslinking by borate leads to low-angle shift

of XRD peaks. The likely cause may be the lattice expansion of semi-crystal region owing to the charge repulsion of tetracoordinated boron.

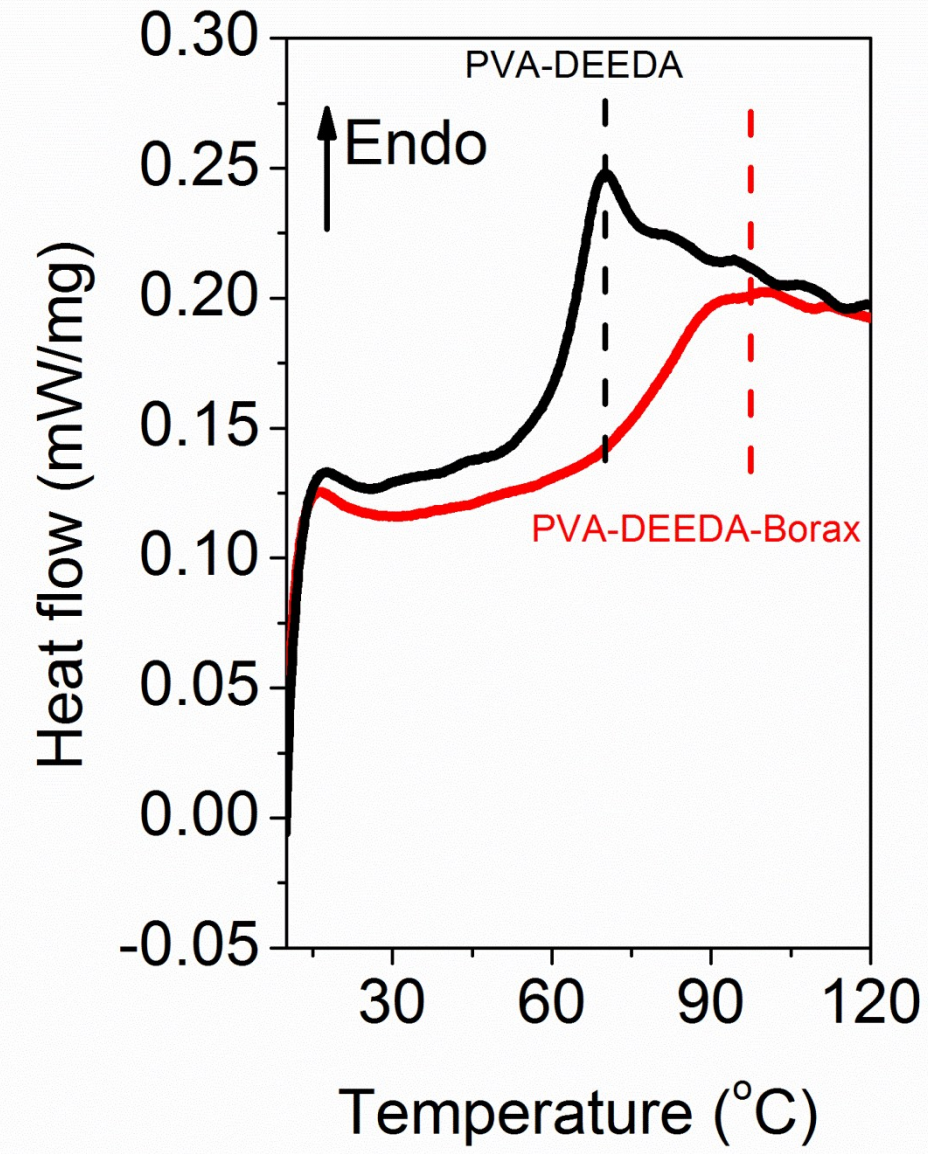

Figure S11. DSC curves of PVA-DEEDA and PVA-DEEDA-Borax film, which is formed upon evaporating the water from PVA-DEEDA-Borax solution. The thermal history was removed before data recording.

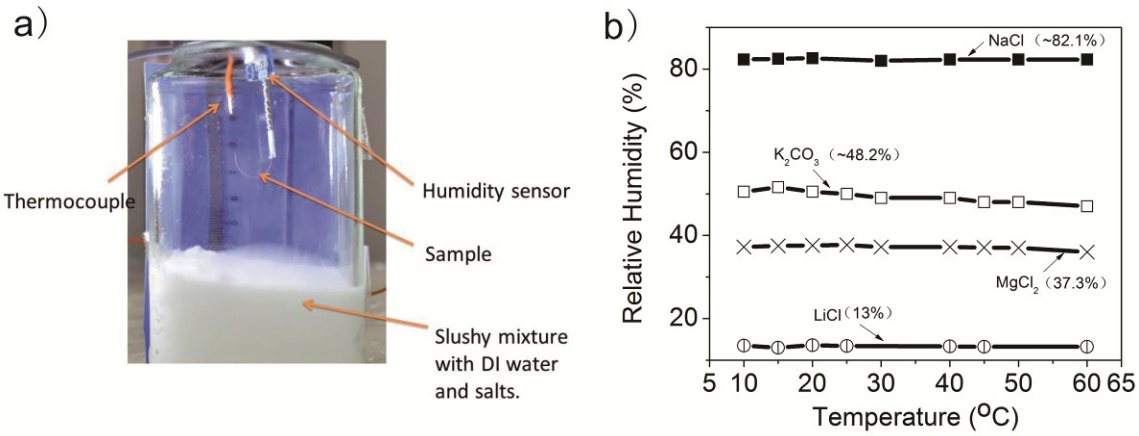

Figure S12. (a) Setup for the bending test and (b) Humidity profile as a function of temperature.

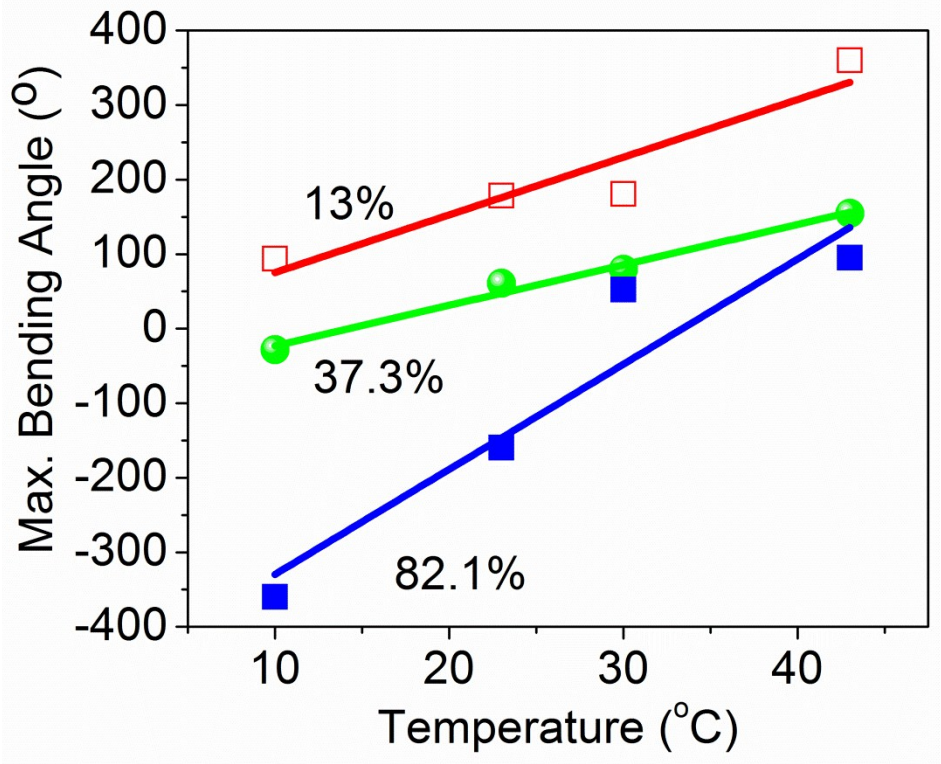

Figure S13. Max bending angle of PVA-DEEDA-Borax based actuator as a function of temperature.

Table S1. Performance comparison between our HA and recently reported state-of-the-art HAs in literatures.

Layer 1	Layer 2	Stimuli	Environment	Max. curvature (mm^{-1})	Ref
pNIPAM (MNP dopped)	PAAm	Temperature (Photo thermal)	Aqueous	12	3
Aligned pNIPAM	Random pNIPAM	temperature	Aqueous	2.6	2a
PAA/PAH	NOA63	Humidity	Humidified air	39.25	4
pNIPAM-NC5	pNIPAM-NC3	temperature	Aqueous	0.65	5
DNA-pNIPAM	DNA-poly(amide)	pH, temperature	Aqueous	18.2	2b
Chitosan (CS) layer	cellulose/CMC layer	pH	Aqueous	15	6
PVA-DEEDA-Borax	**BOPP**	**Moisture, Temperature photothermal**	**Humidified air**	**31.4**	**This work**

Molecular dynamic (MD) simulation:

After the steepest energy minimization, MD simulations of the first 10 ns at 300 K are performed under the NVT ensemble, and the subsequent 20 ns simulations under the NPT ensemble by Berendsen method with a constant pressure of 1.0 bar at 400K. Then the system was further equilibrated for another 20 ns under the NPT ensemble with barostat of Parrinello-Rahman[7] Production MD simulations are performed in stepwise at 4 temperatures (350, 325, 300, 275 K). The simulation time lasts for 40 ns. We use Berendsen thermostat[8] with a time constant of 0.1 ps and Parrinello-Rahman barostat with a time constant of 2.0 ps. The long-range Coulombic interactions are handled by the Particle Mesh Ewald sum method.[9-10] The short-range Lennard Jones terms of the potentials are cut off at 1.2 nm, and the long-range correction terms are added. GROMACS 5.1.1 was used to perform all MD simulations using the generalized amber force field (GAFF).[11-12] TIP3P water model was used.[13]The weight ratio of polymer and water is set as 1:1 based on our experimental study.

Video files:

Movie S1-ESI: Bending test for PVA, PVA-Borax, PVA-DEEDA and PVA-DEEDA-Borax inside a refrigor.

Movie S2-ESI: Bending test for PVA, PVA-Borax, PVA-DEEDA and PVA-DEEDA-Borax inside a hot oven.

Movie S3-ESI: Transformation of actutor as triggered by IR light.

Movie S4-ESI: Artificial muscle demonstration.

Movie S5-ESI: Smart manipulator demonstration.

References

1. (a) M. Amjadi, M. Sitti, High-Performance Multiresponsive Paper Actuators. *ACS Nano* **2016,** *10*, 10202; (b) C. Wen-Hwa, M. Mehregany, R. L. Mullen, Analysis of tip deflection and force of a bimetallic cantilever microactuator. *J. Micromech. Microeng.* **1993,** *3*, 4.

2. (a) L. Liu, A. Ghaemi, S. Gekle, S. Agarwal, One-Component Dual Actuation: Poly(NIPAM) Can Actuate to Stable 3D Forms with Reversible Size Change. *Adv.Mater.* **2016,** *28*, 9792; (b) Y. Hu, J. S. Kahn, W. Guo, F. Huang, M. Fadeev, D. Harries, I. Willner, Reversible Modulation of DNA-Based Hydrogel Shapes by Internal Stress Interactions. *J. Am. Chem. Soc.* **2016,** *138*, 16112.

3. D. Kim, H. Kim, E. Lee, K. S. Jin, J. Yoon, Programmable Volume Phase Transition of Hydrogels Achieved by Large Thermal Hysteresis for Static-Motion Bilayer Actuators. *Chem. Mater.* **2016,** *28*, 8807.

4. Y. Ma, Y. Zhang, B. Wu, W. Sun, Z. Li, J. Sun, Polyelectrolyte Multilayer Films for Building Energetic Walking Devices. *Angew. Chem. Int. Ed.* **2011,** *50*, 6254.

5. C. Yao, Z. Liu, C. Yang, W. Wang, X. J. Ju, R. Xie, L. Y. Chu, Poly(N-isopropylacrylamide)-Clay Nanocomposite Hydrogels with Responsive Bending Property as Temperature-Controlled Manipulators. *Adv. Funct. Mater.* **2015,** *25*, 2980.

6. J. Duan, X. Liang, K. Zhu, J. Guo, L. Zhang, Bilayer hydrogel actuators with tight interfacial adhesion fully constructed from natural polysaccharides. *Soft. Matter* **2017,** *13*, 345.

7. Parrinello, M.; Rahman, A. Polymorphic transitions in single crystals: A new molecular dynamics method. J. Appl. Phys. 1981, 52 (12), 7182-7190.

8. Berendsen, H. J. C.; Postma, J. P. M.; van Gunsteren, W. F.; DiNola, A.; Haak, J. R. Molecular dynamics with coupling to an external bath. J. Chem. Phys. 1984, 81 (8), 3684-3690.

9. Darden, T.; York, D.; Pedersen, L. Particle mesh Ewald: An N·log(N) method for Ewald sums in large systems. J. Chem. Phys. 1993, 98 (12), 10089-10092.

10. Essmann, U.; Perera, L.; Berkowitz, M. L.; Darden, T.; Lee, H.; Pedersen, L. G. A smooth particle mesh Ewald method. J. Chem. Phys. 1995, 103 (19), 8577-8593.

11. Van Der Spoel, D.; Lindahl, E.; Hess, B.; Groenhof, G.; Mark, A. E.; Berendsen, H. J. C. GROMACS: Fast, flexible, and free. J. Comput. Chem. 2005, 26 (16), 1701-1718.

12. Wang, J.; Wolf, R. M.; Caldwell, J. W.; Kollman, P. A.; Case, D. A. Development and testing of a general amber force field. J. Comput. Chem. 2004, 25 (9), 1157-1174.

13. Jorgensen, W. L.; Chandrasekhar, J.; Madura, J. D.; Impey, R. W.; Klein, M. L. Comparison of simple potential functions for simulating liquid water. J. Chem. Phys. 1983, 79 (2), 926-935.